Local magnetism in the molecule-based metamagnet $[Ru_2(O_2CMe)_4]_3[Cr(CN)_6]$ probed with implanted muons

Tom Lancaster,[1,*] Francis L. Pratt,[2] Stephen J. Blundell,[1] Andrew J. Steele,[1] Peter J. Baker,[2] Jack D. Wright,[1] Isao Watanabe,[3] Randy S. Fishman,[4] and Joel S. Miller[5]

[1]*Oxford University Department of Physics, Clarendon Laboratory, Parks Road, Oxford, OX1 3PU, United Kingdom*
[2]*ISIS Facility, STFC Rutherford Appleton Laboratory, Chilton, Oxfordshire OX11 0QX, United Kingdom*
[3]*Muon Science Laboratory, RIKEN, 2-1 Hirosawa, Wako, Saitama 351-0198, Japan*
[4]*Materials Science and Technology Division, Oak Ridge National Laboratory, Oak Ridge, Tennessee 37831-6453, USA*
[5]*Department of Chemistry, University of Utah, Salt Lake City, Utah 84112-0850, USA*

(Received 16 August 2011; published 30 September 2011)

We present a muon-spin relaxation study of local magnetism in the molecule-based metamagnet $[Ru_2(O_2CMe)_4]_3[Cr(CN)_6]$. We observe magnetic order with $T_N = 33$ K, although above 25 K the sublattice spins become less rigid and a degree of static magnetic disorder is observed. The comparison of measurements in applied magnetic field with simulations allows us to understand the origin of the muon response across the metamagnetic transition and to map out the phase diagram of the material. Applied hydrostatic pressures of up to 6 kbar lead to an increase in the local magnetic field along with a complex change in the internal magnetic-field distribution.

DOI: 10.1103/PhysRevB.84.092405 PACS number(s): 76.75.+i, 75.50.Xx, 75.50.Ee

Molecule-based magnets are comprised of arrays of magnetic ions linked with molecular building blocks that form the exchange paths that lead to collective behavior.[1] The molecule-based magnet $[Ru_2(O_2CMe)_4]_3[Cr(CN)_6]$ (hereafter $[Ru_2]_3[Cr]$) is an interesting system based on two interpenetrating magnetic sublattices.[2–5] Each cubic sublattice consists of $S = \frac{3}{2}$ $[Cr(CN)_6]^{3-}$ ions (hereafter [Cr]) at the corners of the cube with $S = \frac{3}{2}$ $[Ru_2(O_2CMe)_4]^+$ ions (hereafter $[Ru_2]$) bridging pairs of [Cr] ions. A second identical sublattice is displaced by half a body diagonal from the first, creating the interpenetrating lattice structure.

The physics of this system[4] is controlled by three energy scales. (i) The largest is easy-plane anisotropy D of the Ru_2 dimers, estimated to be $D/k_B \approx 100$ K. (ii) Antiferromagnetic (AF) exchange J between neighboring $[Ru_2]$ and [Cr] groups within a sublattice is estimated to be $J/k_B \approx 20$ K. This couples ions to form a large, rigid, ferrimagnetic sublattice moment of $M_{sl} = 1.21S$ per Cr ion, constrained [as a result of the anisotropy described in (i)] to point along one of the cube diagonal directions $\boldsymbol{n}$. (iii) Weak antiferromagnetic exchange K between the sublattices is estimated to be ~10 mK. The explanation for the magnetic behavior of this system[4] is therefore based on a picture of sublattices possessing large magnetic moments that are constrained by a sizable anisotropy to lie along a cube diagonal [Fig. 1(b)], with a large energy barrier between the different possible orientations of that moment. The collective magnetic behavior is controlled by weak intersublattice coupling.

Magnetic measurements[3,6] show antiferromagnetic order at $T_N = 33$ K, with the sublattice moments antialigned along a cube diagonal (i.e., $\boldsymbol{n}_1 = -\boldsymbol{n}_2$). Below 25 K, applied fields of magnitude $B_c \approx K/\mu_B \approx 100$ mT overcome the weak coupling K between sublattices, causing a metamagnetic transition between the antiferromagnetic state and a state with a paramagnetic component. The net moment of each sublattice (coupled by the large exchange J) is only very weakly perturbed by such small fields, but this assumption breaks down above 25 K where the large sublattice spins are no longer rigid.[6]

To investigate $[Ru_2]_3[Cr]$ from a microscopic point of view, we made muon-spin-relaxation (μ^+SR) measurements[7] in zero applied magnetic field (ZF) and in applied longitudinal field (LF). We have also made measurements in applied hydrostatic pressures of up to 6 kbar. A polycrystalline sample of $[Ru_2]_3[Cr]$ was prepared as described previously.[2] ZF μ^+SR measurements were made at the Swiss Muon Source (SμS) using the DOLLY and GPS spectrometers. Measurements were also made in LF and at applied hydrostatic pressures using the RIKEN-RAL ARGUS spectrometer at the ISIS facility.[8]

Example ZF spectra measured at SμS are shown in Fig. 1(a). Above the magnetic transition at $T_N = 33$ K the spectra are well described by an exponential relaxation function, as expected for a paramagnet with dynamically fluctuating magnetic moments.[9] At the lowest measured temperature of $T = 2$ K a heavily damped oscillation is observed in the time dependence of the muon polarization [the "asymmetry" $A(t)$], which is characteristic of a quasistatic local magnetic field at the muon stopping site. This local field causes a coherent precession of the spins of those muons for which a component of their spin polarization lies perpendicular to this local field. In general, the muon response in a magnetically ordered, polycrystalline material will have the form $A(t) = A_\parallel(t) + A_{osc}(t)$, where $A_\parallel$ accounts for the component of the muon spins parallel to the local magnetic field of the muon site and A_{osc} is the amplitude of the oscillating component (expected to be $\frac{2}{3}$ of the total spin polarization in ZF). The frequency of the oscillations is given by $\nu_i = \gamma_\mu |B_i|/2\pi$, where γ_μ is the muon gyromagnetic ratio ($=2\pi \times 135.5$ MHz T^{-1}) and B_i is the average magnitude of the local magnetic field at the ith muon site. Any spatial or temporal variation in magnitude of these local fields will result in a relaxation of the oscillating signal. The heavy damping of our signal points to a broad distribution of local magnetic fields at the muon site(s) in this material. This is most probably due to the existence of a

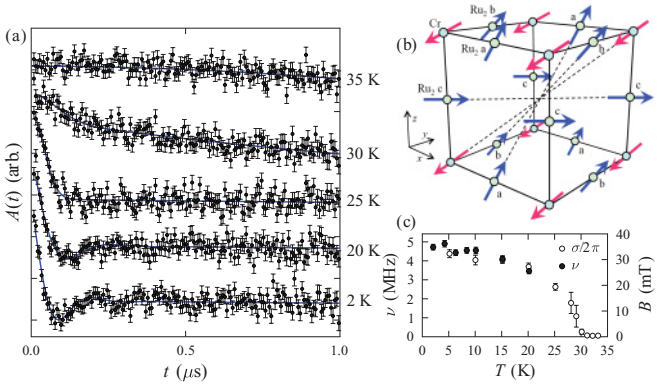

FIG. 1. (Color online) (a) ZF μ^+ SR showing the temperature evolution of the signal for temperatures $2 \leqslant T \leqslant 35$ K. (Spectra have been offset for clarity.) (b) Proposed ground state (Ref. 4) of a single sublattice. (c) Temperature evolution of the muon-spin precession frequency, which ceases to be resolvable above $T \approx 25$ K, and the relaxation rate σ of the fast relaxing component.

relatively broad, static distribution of local magnetic fields at the muon sites in $[Ru_2]_3[Cr]$.

To extract the precession frequency as a function of temperature, spectra were fitted to the function $A(t) = A_1 e^{-\Lambda t} + A_2 e^{-\lambda t} \cos(2\pi \nu t) + A_{bg}$, where the first term corresponds to $A_\parallel$, the second to A_{osc}, and A_{bg} accounts for those muons stopping in the sample holder or cryostat tail. The evolution of the extracted muon precession frequency is shown in Fig. 1(c) for temperatures $T \lesssim 25$ K where a well defined oscillation is observable. The oscillation disappears around 20 K [Fig. 1(a)] and above that temperature the spectra are best described with a purely relaxing function with A_{osc} taking a Gaussian form. These measurements confirm that the material is magnetically ordered throughout its bulk below T_N and show that the average magnetic field at the muon site(s) that give rise to the oscillation tends to ≈39 mT for $T \to 0$. The disappearance of the oscillatory signal above 25 K fits with the suggestion that the sublattice spins lose their rigidity above 25 K. When this occurs the magnetic-field distribution at the muon sites broadens considerably, washing out the oscillations. An alternative analysis procedure involves fitting the spectra to a Gaussian function across the entire temperature range. The resulting relaxation rate σ is shown in Fig. 1(c), where we see that σ tracks the behavior of ν below 25 K and then continuously decreases to zero around T_N, reflecting a continuous decrease in the magnitude of the ordered moment with increasing temperature.

Using the known ground-state magnetic structure[4] we have searched for muon sites based on calculations of the dipole field distribution in the material. A field of 39 mT, corresponding to the oscillation frequency at low temperature, may be found for muon sites displaced 0.183 cell units from a Cr along those six [111] axes that do not lie along the local axis of the Cr moment. For the two sites which lie along the axis of the Cr moment the local field is 111 mT. If the Ru_2 spin is reduced from 1.5 to 1.23, as has been suggested,[4] then the displacement reduces slightly to 0.181 cell units. These sites nestle in between three CN groups, which are highly electronegative and therefore attractive to a positive muon. We note also that this type of muon site is very similar to that suggested for the molecule-based metamagnet[10] $CuW(CN)_8(tetrenH_5)_{0.8}\cdot 7H_2O$, which shares several common features.

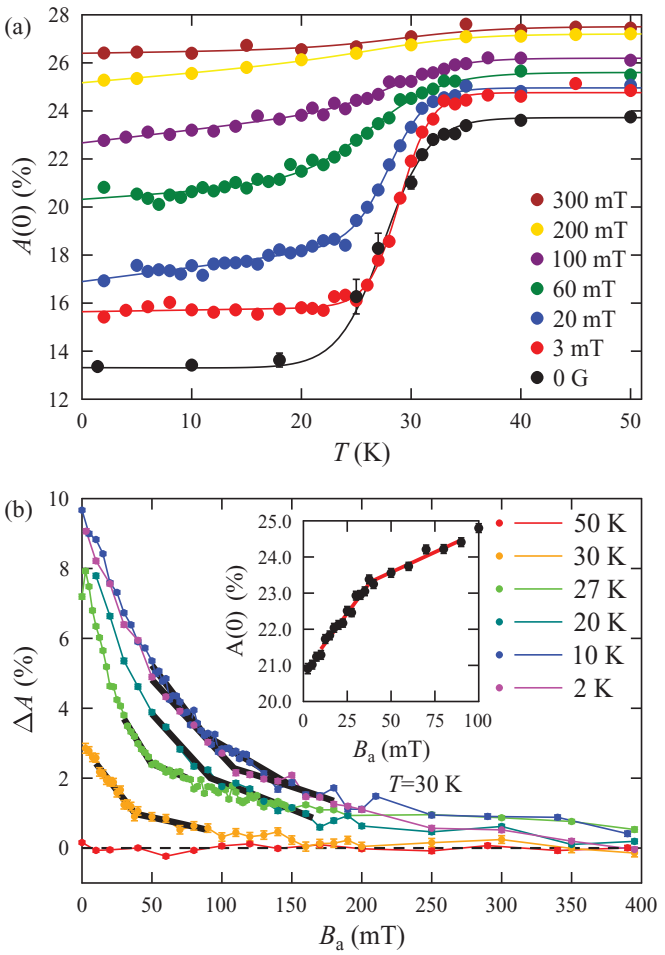

FIG. 2. (Color online) (a) The evolution of the initial asymmetry $A(0)$ with temperature at applied LFs. (b) Evolution of $\Delta A (\propto A_{osc})$ with LF at several temperatures. Lines are guides to the eye showing the positions of changes in slope we identify with magnetic transitions. Inset: Detail of measurement of $A(0)$ made at 30 K showing a typical transition.

To map out the B-T phase diagram, complementary data were measured at the ISIS facility with magnetic fields B applied longitudinal to the initial direction of the muon spin. The muon pulse at ISIS (Refs. 11 and 12) has a width τ_{mp}≈80 ns, limiting the response to frequencies above $\approx\tau_{mp}^{-1}$. Owing to this limitation on the ISIS time resolution we expect to observe full asymmetry above the magnetic transition at T_N but only the component $A_\parallel$ well below T_N, resulting in an apparent decrease in the initial amplitude $A(t = 0)$ as the material is cooled through T_N. The measured initial asymmetry amplitude $A(0)$ is plotted in Fig. 2(a) as a function of temperature at fixed magnetic field. In small applied fields we observe a decrease in $A(0)$ below $T_N = 33$ K. The transition region is quite broad, with $A(0)$ only reaching a constant value below 25 K. This is in keeping with the ZF results discussed above, where oscillations were not resolvable in the $25 < T < T_N$ region due to the melting of the rigid sublattice spin arrangement. The

amplitude transition is seen to become broader with increasing applied field, with the high-temperature onset shifting to higher temperatures and the region of flattening off at low temperature shifting to lower temperatures. This suggests that an applied field leads to a increase in the temperature range over which the spins within a sublattice have a degree of independence.

To probe the metamagnetic transition, scans in applied magnetic field at fixed temperature were made. As shown in the inset to Fig. 2(b) a discontinuous change in gradient is observed in these scans, whose position correlates with the metamagnetic transitions previously observed.[6] Data in Fig. 2(b) show ΔA, which is the difference in $A(t = 0)$ between 50 K (well above T_N) and 2 K (well below T_N). This quantity is proportional to A_{osc}. The transitions we identify lie at slightly higher fields than those identified from magnetization and the discontinuities are most clear in the data measured above the sublattice melting point of ~25 K.

The decrease of ΔA with LF arises because a field B directed along the initial muon spin locks a fraction of the muons along this direction, reducing the extent of the relaxation caused by the internal field at the muon site and hence A_{osc}. In a polycrystalline, statically ordered magnet with a unique muon site A_{osc} (and therefore ΔA) is expected to follow,[10]

$$A_{osc} = \frac{1}{4} + \frac{1}{4b^2} - \frac{(b^2-1)^2}{8b^3} \ln\left|\frac{b+1}{b-1}\right|, \qquad (1)$$

where $b = B/B_0$ and B_0 is the size of the static internal field at the muon site in the absence of the applied field B. In order to further understand how the field dependence of ΔA corresponds to the underlying change in magnetic configuration at the metamagnetic transition, numerical simulations were performed using the effective model of the system developed previously by Fishman and co-workers.[4,5,13] We calculate the probability distribution of the 64 possible sublattice configurations, whose energies are given in the model by $E = N_{Cr} \sum_i [-\mu_B M_{sl}(\boldsymbol{n}_{1i} + \boldsymbol{n}_{2i}) \cdot \boldsymbol{B} + 3KS^2 M_{sl}^2 \boldsymbol{n}_{1i} \cdot \boldsymbol{n}_{2i}]$, where the sum is over clusters, each containing N_{Cr} unit cells. We use the identical parameters that were found to best describe the experimental data from the previous work.[4,5,13] For each muon site that we have identified we also calculate the distribution of dipole fields for muons for each sublattice configuration. Combined with the probability distribution for the configurations this provides a distribution of local fields experienced by the muon ensemble, which is used to evaluate A_{osc}. A comparison of the predicted behavior and experimental results at 1.8 K is shown in Fig. 3(a) where the solid line shows the simulated result after polycrystalline averaging. The simulated result is seen to describe the experimental data quite well and shows a pronounced change in gradient around 100 mT corresponding to the metamagnetic transition. A slightly better description of the data is achieved if we assume an incomplete angular averaging. The dashed line in Fig. 3(a) shows the result for a field oriented along a line joining the center of the unit cell and the middle of a cube edge. This simulation reproduces a small anomaly visible in our data, and does so at slightly higher field than the change in gradient predicted by the polycrystalline calculation. The better description of the data provided by this orientation leads us to suggest that the crystals in our experiments have some

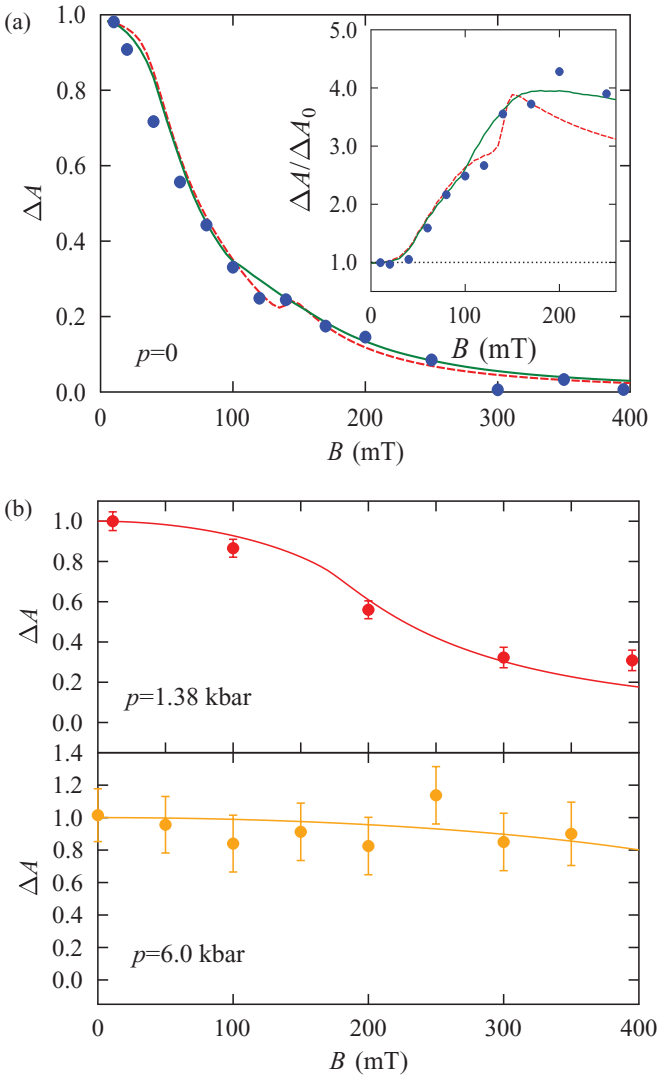

FIG. 3. (Color online) (a) Zero pressure behavior for ΔA compared with simulations. Inset: ΔA normalized by the prediction of Eq. (1) for a single site with $B_0 = 39$ mT. (b) Pressure dependence of ΔA as a function of applied magnetic field. The lines represent fits described in the text.

degree of this alignment, possibly caused by the applied field. This would also explain why the discontinuities identified in our measurements of ΔA shown in Fig. 2(b) lie slightly higher in field than the previously identified metamagnetic transitions. The inset to Fig. 3(a) shows the measured result and the results of both simulations normalized by the prediction of Eq. (1) for a single internal field of 39 mT (suggested by the low-temperature limit of our measured ZF precession frequency). We see a substantial deviation from the prediction of Eq. (1) for both the measurements and the simulations (with the metamagnetic transition seen clearly as a rapid increase in the measured points and the simulation of the aligned system), demonstrating that the behavior of the system certainly cannot be captured by a simple non-metamagnetic model involving a single site.

A phase diagram summarizing the results of our measurements is shown in Fig. 4. We are able to identify the metamagnetic transition shown by a solid line, which separates

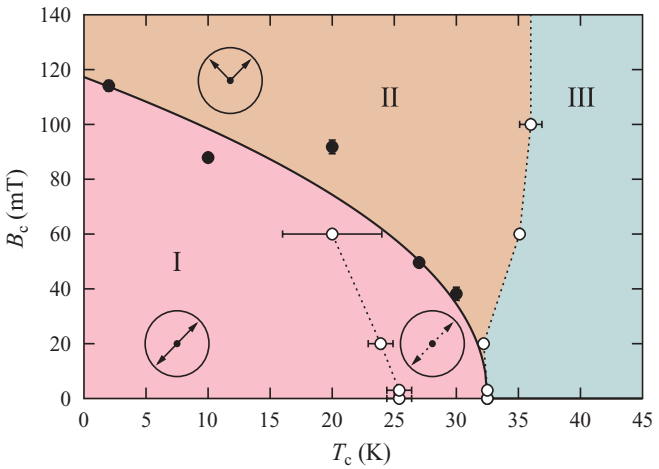

FIG. 4. (Color online) Notional phase diagram at ambient pressure derived from our measurements (see main text).

region I, the antiferromagnetic regime, and region II, where the rigid sublattice spins are flipped by the applied field to point along another cube diagonal. At high temperature is region III, which is a phase where all spins are disordered. The dotted lines represent the transition region where the asymmetry ΔA measured as a function of temperature in fixed field changes rapidly. In the region between these dotted lines, centered around 30 K, the sublattice spins are less rigid. For $B = 0$ this corresponds to Gaussian muon-spin relaxation and an absence of oscillations, implying that the local-field distribution in this region is quasistatic but has a significant degree of disorder compared to the more ordered local field in the rest of region I. The nature of the field induced transition in this region might be expected therefore to be rather different than that observed below 25 K.

Finally, we have investigated the effect of pressure[14] on the local magnetism in $[Ru_2]_3[Cr]$ through measurements as a function of longitudinal magnetic field at several applied hydrostatic pressures. μ^+SR data measured using a Cu-Be pressure cell is shown in Fig. 3(b). We expect the application of pressure to increase the size of the sublattice moments by enhancing the exchange coupling J between [Cr] and $[Ru_2]$ spins.[5] This should manifest itself in our data in terms of a ΔA, which becomes more robust against applied magnetic field under pressure, reflecting the greater relaxation of the muon spins caused by the increased internal field. This is indeed what we measure, with ΔA showing less decrease with applied field with increasing values of pressure. By 6 kbar the maximum achievable applied field (400 mT) has very little effect on ΔA. We also note that, within experimental uncertainty, there is no discernible change in the transition temperature at this pressure.

A crude parametrization of these data may be carried out using Eq. (1). Fitting this to the ambient pressure data [Fig. 3(a)] below the metamagnetic transition at $\approx$120 mT (for $T = 2$ K) yields $B_0 = 39(1)$ mT in good agreement with the value of from the precession frequency at 2 K. Fitting Eq. (1) to the $p > 0$ data yields $B_0 = 170 \pm 80$ mT at 1.38 K increasing to $B_0 = 400 \pm 170$ mT at 6 kbar. It is, however, very unlikely that these values of B_0 represent the true internal fields at the muon site. Previous pressure studies[5] suggest that, at 8 K, the net magnetization of the sublattice increases only from $3.6\mu_B$ to $4.4\mu_B$ in 5.46 kbar. This, and the change in shape of the field evolution of ΔA with increasing pressure is especially seen in the 3-kbar data, suggesting that the nature of the local magnetic-field distribution changes quite dramatically in applied pressure. The application of pressure is expected not only to increase the sublattice moment via an increase in J but also to change the intersublattice coupling K in a nontrivial manner.[5] There is also expected to be a change in the size of magnetically correlated clusters in the material, which will act to change the local-field distribution. It is therefore very likely that the effect of pressure at the level of local fields is more complicated than is currently accounted for in the effective model of this material.

Part of this work was performed at the SμS, Paul Scherrer Institut, Switzerland and at the ISIS Facility, Rutherford Appleton Laboratory, UK using the RIKEN-RAL beamline. We are grateful to Alex Amato and Robert Scheuermann for experimental support. This work was supported by EPSRC (UK), the US NSF (DMR-11063630), and the US Department of Energy, Office of Basic Energy Sciences, Material Sciences and Engineering Division.

*t.lancaster1@physics.ox.ac.uk

[1] S. J. Blundell and F. L. Pratt, J. Phys.: Condens. Matter **16**, R771 (2004).
[2] Y. Liao, W. W. Shum, and J. S. Miller, J. Am. Chem. Soc. **124**, 9336 (2002).
[3] J. S. Miller, T. E. Vos, and W. W. Shum, Adv. Mater. **17**, 2251 (2005).
[4] R. S. Fishman, S. Okamoto, W. W. Shum, and J. S. Miller, Phys. Rev. B **80**, 064401 (2009).
[5] R. S. Fishman, W. W. Shum, and J. S. Miller, Phys. Rev. B **81**, 172407 (2010).
[6] W. W. Shum, J. N. Schaller, and J. S. Miller, J. Phys. Chem. C **112**, 7936 (2008).
[7] S. J. Blundell, Contemp. Phys. **40**, 175 (1999).
[8] I. Watanabe *et al.*, Physica B **404**, 993 (2009).
[9] R. S. Hayano, Y. J. Uemura, J. Imazato, N. Nishida, T. Yamazaki, and R. Kubo, Phys. Rev. B **20**, 850 (1979).
[10] F. L. Pratt, J. Phys.: Condens. Matter **19**, 456207 (2007).
[11] G. H. Eaton *et al.*, Nucl. Instrum. Methods Phys. Res. A **342**, 319 (1994).
[12] P. J. C. King *et al.*, Physica B **326**, 260 (2003).
[13] R. S. Fishman and J. S. Miller, Phys. Rev. B **83**, 094433 (2011).
[14] W. W. Shum, J.-H. Her, P. W. Stephens, W. Lee, and J. S. Miller, Adv. Mater. **19**, 2910 (2007).